Pattern formation in active cytoskeletal networks

R. Peter, V. Schaller, F. Ziebert‡ and W. Zimmermann

Theoretische Physik I, Universität Bayreuth, D-95440 Bayreuth, Germany

E-mail: `Walter.Zimmermann@uni-bayreuth.de`

Abstract. We present a one-dimensional model combining two of the main features of active biopolymer solutions that are only recently investigated experimentally, namely the molecular motor driven active transport of filaments and the (visco-)elastic properties of filament networks held together by crosslinkers or entanglement effects. It is shown that the pattern forming mechanisms, associated to the motor-mediated transport of filaments, are substantially altered when coupled to a filament network: in case of a permanent network, the long-range clustering of filaments changes either to stationary periodic filament density patterning or to propagating pulses. If the network is however viscoelastic, molecular motor activity can lead to traveling or standing filament density waves.

Submitted to: *New J. Phys.*

‡ Present address: Laboratoire de Physico-Chimie Théorique, UMR CNRS 7083, ESPCI, 10 rue Vauquelin, F-75231 Paris cedex 05, France

1. Introduction

The cytoskeleton of eukaryotic cells is constituted of filaments, actin and microtubules, and relies vastly on its ability to actively reorganize itself by polymerization processes and motor protein complexes [1, 2]. The latter active, nonequilibrium process has become a rapidly growing field of research: in reconstituted filament-motor bundles, contracted states and spontaneous oscillations have been found [3, 4, 5]. In extended systems and in the dilute limit, the intermittent motor mediated filament transport leads to spontaneous self-organization [6, 7, 8, 9, 10, 11].

A second important feature of biopolymers is that upon increasing filament densities, elastic networks and gels may be formed either by entanglement effects or by means of permanently crosslinking proteins. During recent years continuous research efforts, both on the experimental and theoretical side, have been devoted to the elastic and dynamic properties of such viscoelastic networks without motor activity [12, 13, 14, 15, 16, 17]. Lately the interplay between active motor transport and an elastic network has been started to be experimentally addressed [18, 19], as well as the influence of a trace amount of crosslinks (not sufficient to build up an interconnected network) on the pattern formation processes [20, 21, 22]. Whereas the motor-mediated transport of filaments as well as passive networks have already been addressed separately to quite some extent, theoretical efforts to join both vitally important features have been started only recently [9, 23]. Understanding such active crosslinked gels would not only be of obvious biological interest, it also comprises a hitherto unexplored material class, that could be called an "active elastomer": liquid crystalline filament ordering is known to appear in biopolymer solutions at sufficiently high densities [24]. Crosslinking a dense ordered filament solution to a gel results in a passive elastomer that has already been recently discussed in case of actin in Ref. [25]. Even more tantalizing is that the temporary action of molecular motors in the biopolymer gel should interplay with the known properties of classical liquid crystalline elastomers [26] composed of crosslinked but passive mesogenic polymers.

Another revealing interpretation of the considered active biological gels, whether elastic or viscoelastic, is the mechanosensitivity of the structures formed: filament-motor systems are known to display various nontrivial patterns [6, 7, 11, 10, 20] whose onsets and characteristics will, in the presence of a network/gel elasticity, naturally be coupled to the network's density and elasticity. The formed structures can thus be regulated by external compression or dilation of the network, an attribute of possible biological relevance, e.g. in cell mechanotransduction, not discussed so far.

Aiming at the description of active biogels, in the present work we introduce a simple one-dimensional model based on a mean-field description of active filament bundles [4, 5] coupled to a continuum description of an isotropic, either elastic or viscoelastic network. Despite its simplicity, the analysis of this model in the geometry of a polar bundle gives already rise to phenomena expected to persevere in two- and three-dimensional actin networks and gels: contracted states, which are known from muscle bundles, become

oscillatory due to the coupling of active transport to network elasticity. Second, changing the network from elastic to viscoelastic, leads to a switching from solitary propagating filament density profiles to extended traveling or standing waves - the latter might be of relevance for cell locomotion. Moreover, all these processes additionally are mechanosensitive. We also discuss how the model has to be generalized to become more realistic, e.g. by accounting for an exchange of filaments in solution and in the network, as well as for anisotropic networks.

2. Model for an active filament network

A solution of cytoskeletal filaments forms networks in the presence of crosslinkers §, which are actively reorganized and set under stress in the presence of motors. To get a treatable model for such a complex system, several approximations have to be made. One assumption we use here is that the average crosslinking time is large compared to the average runlength of the motors on filaments. In this limit, it is appropriate to divide the total filament density into a fluid part, made up of filaments not in permanent contact with the network and either moved by molecular motors or randomly (referred to as 'free' filaments hereafter) and into an elastic part supposed to be formed of crosslinked filaments, which form a (visco-)elastic network ('network' filaments). This approach is related to two-fluid models [27, 28], well known for complex fluids. To overcome the limit of permanent crosslinkers, one can account for transition rates between free and network filaments, as will be done in the future. Such transition kinetics is known to favor spatially periodic patterns in related systems, e.g. self-assembling biofilaments [29]. For a one-to-one experimental realization of this model, one can imagine an *in vitro system* where crosslinking times much longer than *in vivo* are achieveable, or even use artificial crosslinks.

A second approximation made - which however has no effect on the simplest case of a perfectly polar bundle solely investigated in this work - is that the network itself remains perfectly isotropic. The *total* filament system (i.e. free and network filaments together) may however become anisotropic upon the reorganization of the free filaments. We discuss this approximation in more detail below.

To highlight the new properties due to the (visco-)elastic background we will consider the simplest case of a one-dimensional system, i.e. an active filament bundle structure. We use an approach commonly accepted in the literature for one-dimensional motor-filament solutions without (visco-)elastic background [4, 5, 30]‖. Thereby the free filament bundle axis is referred to as the x-direction. Since free filaments are polar with respect to the action of molecular motors, an active free filament bundle is distinguished

---

§ Upon increasing the filament density to the semidilute regime, entanglement effects also lead to the formation of networks and gels. Here we concentrate however on the crosslinked case, since our modeling is restricted to the dilute regime.

‖ The generalization of the aforesaid models to higher dimensions is principally known [8, 10, 11] and the influence of an elastic network in higher dimensions will be investigated in forthcoming work.

by number densities $c^+(x)$ and $c^-(x)$ of filaments with their plus ends pointing either in positive or negative x-direction. As the (visco-)elastic network is as well composed of filaments, it *locally* can be described by a second class of filament number densities, $d^\pm(x)$. While motor induced interactions among network filaments are neglected due to their large meshsize, motors may couple network filaments to free filaments (just as like they couple free filaments). Therefore free filaments can be actively transported along the network in addition to active transport of free filament pairs. The d-filaments will be used to define the interactions between the free filaments and the network. On large scales however the network dynamics is best captured by a one-dimensional displacement variable $u(x)$. To get a closed set of equations the spatial modulations of the d-filament number density around its mean value d_0 will be expressed in terms of $u(x)$, yielding coupled equations for the 'free' filament density profiles and the displacement variable.

Assuming filaments with a fixed length ℓ, the dynamics of the 'free' filaments is governed by conservation laws

$$\partial_t c^\pm = D\,\partial_x^2 c^\pm - \partial_x J^\pm \tag{1}$$

wherein D is an effective diffusion coefficient. Provided that two–filament interactions are prevalent (corresponding to a low motor density or duty ratio), the motor–induced currents incorporate both the interactions between free filaments and the interaction of a free and a network filament. This leads to the decomposition $J^\pm = J_1^\pm + J_2^\pm + J_u^\zeta$, where $J_1^\pm$ stands for interactions between free filaments and $J_2^\pm$ for free filament/network interactions respectively. As it is derived later, J_u^ζ is caused by frictional effects the biopolymer network exerts on the free filaments. Both currents $J_{1,2}^\pm$ can be derived from micro-force balance, as it has been done in [30] for the interaction of free filaments, which suggests the currents $J_1^\pm = J_{cc}^{\pm\pm} + J_{cc}^{\pm\mp}$ to be

$$J_{cc}^{\pm\pm} = \alpha \int_0^\ell d\xi \, \left[c^\pm(x+\xi) - c^\pm(x-\xi) \right] \, c^\pm(x), \tag{2a}$$

$$J_{cc}^{\pm\mp} = \mp\beta \int_{-\ell}^\ell d\xi \, c^\mp(x+\xi)\,c^\pm(x). \tag{2b}$$

Here α and β are averaged cross–sliding velocities characterizing the interaction strength of parallel and antiparallel filaments. On larger scales, the α-contributions favor stationary contracted states of filaments, while the β-contributions lead to a phenomenon called polarity sorting, and also to propagating solitary density modes [4, 5, 31]. Since the free filaments both are exposed to the same local restoring force - namely the friction with the surrounding fluid - the center of mass of a free filament pair is invariant.

This however does not hold, if a network filament interacts with a free filament: different restoring forces, the aforementioned frictional force and the elastic contribution in the case of the network filament, lead to an effective barycentric transport, as it can be seen from Fig. 1. The displacement of the center of mass is equivalent to an additional

current J_u^χ, yielding $J_2^\pm = J_{dc}^{\pm\pm} + J_{dc}^{\pm\mp} + J_u^\chi$, wherein

$$J_{dc}^{\pm\pm} = \alpha \int_0^\ell d\xi \left[d^\pm(x+\xi) - d^\pm(x-\xi) \right] c^\pm(x), \tag{3a}$$

$$J_{dc}^{\pm\mp} = \mp\beta \int_{-\ell}^\ell d\xi \, d^\mp(x+\xi) c^\pm(x), \tag{3b}$$

are the natural extensions of Eqs. (2) for motor-mediated interactions between $d^\pm$- and $c^\pm$-filaments. The current J_u^χ is given by

$$J_u^\chi = \int_{-\ell}^\ell d\xi \left[\frac{\chi}{\eta} \left[(\lambda + 2\mu) + \tau\partial_t \right] \partial_x^2 u(x+\xi) \right] d(x+\xi) \, c^\pm(x). \tag{4}$$

It makes allowance for the fact that the viscoelastic force density $\left[(\lambda + 2\mu) + \tau\partial_t \right] \partial_x^2 u$ enters the microscopic force balance, when an active overlap between a network filament and a free filament is met. This can also be derived from microscopic force balance as it is made plausible in Appendix A. Another aspect which has to be taken into account is the frictional interaction between free filaments and the network as a whole if the network slides by at a velocity $\partial_t u(x)$. This is done by the contribution

$$J_u^\zeta = -\zeta \, \ell \left[\partial_t u(x) \right] d(x) c^\pm(x) \tag{5}$$

with $\zeta = \zeta'/\eta$. The dynamic equations for the free filaments then read

$$\partial_t c^\pm = D \, \partial_x^2 c^\pm - \partial_x \left(J_{cc}^{\pm\pm} + J_{cc}^{\pm\mp} + J_{dc}^{\pm\pm} + J_{dc}^{\pm\mp} + J_u^\chi + J_u^\zeta \right). \tag{6}$$

As aforementioned the dynamics of the (visco-)elastic network, locally constituted of the $d^\pm$-filaments, is best described by a displacement variable $u(x)$. Force balance then implies $\partial_x \sigma + f = 0$ with σ an appropriate stress and f a force density yet to be defined. The force density f comprises the frictional force density $-\gamma\partial_t u$ due to network frictions with the surrounding solvent, the drag force density f_c^{drag} accounting for the change in friction induced by the active free filament currents and the motor mediated driving force density f_u resulting from interactions between free and network filaments. This yields

$$\gamma\partial_t u = f_c^{\mathrm{drag}} + f_u + \partial_x \sigma, \tag{7}$$

where γ denotes the viscous friction coefficient between the network and the surrounding solvent that in principle depends on the three dimensional morphology of the network but is considered to be a constant in our one dimensional model ¶. The stress σ can be decomposed into $\sigma = \sigma^{\mathrm{E}} + \sigma^{\mathrm{F}}$. σ^{E} stems from the elastic network deformations characterized by $\partial_x \sigma^{\mathrm{E}} = (\lambda + 2\mu) \partial_x^2 u$ with Lamé coefficients λ and μ. τ being a friction coefficient, the frictional contribution $\sigma^{\mathrm{F}} = \tau\partial_x\partial_t u$ to the total stress σ accounts for frictions *within* the elastic network [32, 33]. According to the Voigt-Kelvin body [34] the fraction $(\lambda + 2\mu)/\tau$ then defines a time constant governing the formation/relaxation of strain within the network if an external force is applied/released. Network dynamics

¶ Inertia effects are also neglected, since the network's mass density covers only a small fraction of the systems total mass and the solvent-viscosity is large.
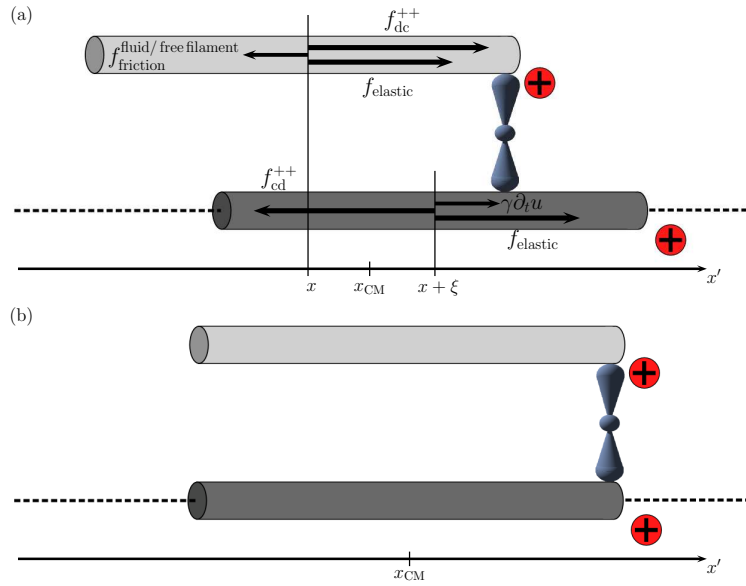
Figure 1. (*a*) Schematic representation of the forces exerted by a motor complex between a free filament (light gray shaded) and a network filament (dark gray shaded) of the same orientation. (*b*) In contrast to interacting free filament pairs, the center of mass x_{CM} of the free/network filament pair is displaced if a molecular motor has actively coupled the considered filaments. The microscopic forces depicted in (*a*) result in an effective barycentric transport of the free filament whose center of mass is shifted from x to x_{CM} while the network filament's center of mass is hardly affected. The barycentric transport of the free filament that gives rise to the current J_u^χ strongly depends on the viscoelastic force density $f_{\mathrm{elastic}} = [(\lambda + 2\mu) + \tau\partial_t]\,\partial_x^2 u$.

is governed by the following dynamical equation for the network's displacement variable $u(x)$

$$\gamma\,\partial_t u = [\,(\lambda + 2\mu) + \tau\,\partial_t\,]\,\partial_x^2 u + f_u + f_c^{\mathrm{drag}}\,. \tag{8}$$

In analogy to $J^\pm$, the force density f_u originating from the motor-mediated interaction between free and network filaments reads $f_u = f_{cd}^{++} + f_{cd}^{--} + f_{cd}^{-+} + f_{cd}^{+-}$, with

$$f_{cd}^{\pm\pm} = \alpha\,\eta\,\ell\int_0^\ell d\xi\,\left[c^\pm(x+\xi) - c^\pm(x-\xi)\right]d^\pm(x)\,, \tag{9a}$$

$$f_{cd}^{\mp\pm} = \mp\beta\,\eta\,\ell\int_{-\ell}^\ell d\xi\,c^\mp(x+\xi)\,d^\pm(x)\,, \tag{9b}$$

Here η is the friction coefficient a free filament experiences if moved through the surrounding solvent. The free filament currents given by Eqs. (2) acting on the network filaments alter the drag force $-\gamma\partial_t u$ according to

$$f_c^{\mathrm{drag}} = \nu\ell\left(J_{cc}^{++} + J_{cc}^{--} + J_{cc}^{+-} + J_{cc}^{-+}\right) \tag{10}$$

with ν denoting an adequate friction coefficient.

In order to get a closed set of equations, the spatial variation of the density $d(x)$ needs to be interpreted in terms of the displacement field $u(x)$. As the local density $d(x)$

is increased in regions where the displacement field $u(x)$ changes from high to low values and vice versa, spatial modulations of $d(x)$ are proportional to $\partial_x u(x)$ which allows the network density to be approximated (to leading order) by

$$d^+(x) = d^-(x) = d(x)/2 = (d_0 - \delta \partial_x u)/2. \tag{11}$$

The parameter δ relates the spatial modulation of the network filament density $d(x)$ around its mean value d_0 to the displacement field $u(x)$.

In Eq. (11), we have made the approximation that the network itself remains perfectly isotropic (i.e. $d^+(x) = d^-(x)$). In the general one-dimensional case, the local difference between the plus and minus filaments can be in principle nonzero, leading to an anisotropy. For this reason, one has to keep in mind that we deal with a coarse-grained model, which is valid only on length scales above several filament lengths, and that the network is tightly crosslinked, so that plus and minus filaments incorporated in the network can not be moved independently as in the case considered originally in [5]. If the network is deformed and relaxes, due to the tight crosslinking the filaments of the two possible directions, plus and minus, both locally undergo approximately the same displacements. In the two- or three-dimensional case, Eq. (11) has to be generalized. In one dimension, anisotropy can be generated if - for a finite crosslinking time - transitions between network and free filaments are included, as will be discussed in future work.

To study now the essential effects of the network on the free filament dynamics, we consider in the following a perfectly polar bundle by setting $c^-(x) = d^-(x) = 0$. Consequently $d^+(x)$ passes into $d(x) = d_0 - \delta \partial_x u(x)$. The free plus-filaments with density $c^+(x)$ are denoted by $c(x)$ hereafter. In the absence of a network the system is then known to trigger a subcritical, long-wavelength bifurcation to contracted states [5]. In the remaining chapters we show that both an elastic and a viscoelastic network significantly alter the pattern forming processes in motor-filament systems: the modified model already allows for oscillatory instabilities, even though there are no antiparallel interactions present, as well as for pattern forming instabilities with finite wavelength.

3. Patterns in an active elastic bundle.

In case of an elastic network, i.e. $\tau = 0$, the equations of the previous section reduce to

$$\partial_t c \quad = D\partial_x^2 c - \partial_x \left(J_{cc}^{++} + J_{dc}^{++} + J_u^{\zeta} + J_u^{\chi} \right), \tag{12a}$$

$$\gamma \, \partial_t u = (\lambda + 2\mu) \, \partial_x^2 u + f_{cd}^{++} + \nu \ell J_{cc}^{++}. \tag{12b}$$

These equations are rescaled by introducing dimensionless coordinates $x' = x/\ell$ and $t' = tD/\ell^2$, normalized density $c^{+'} = \ell c^+$ and displacement variable $u' = u/\ell$, as well as $\alpha' = (\alpha \, \ell)/D$, $\delta' = \ell \, \delta$, $\eta' = \eta/\gamma$, $\nu' = \nu/\gamma$ $d_0' = \ell d_0$ and $E = (\lambda + 2\mu)/(\gamma D)$ for the elastic modulus. The primes are omitted for the sake of simplicity.

The nonlinear integro-differential Eqs. (12) are analyzed for a system of length L with periodic boundary conditions. The stability of the spatially homogeneous basic state, corresponding to a filament density $c(x) = c_0$ and a vanishing (or constant) displacement field $u(x) = 0$, can be analyzed by linearizing Eqs. (12) around this state,

$c(x) = c_0 + \sum_k c_k(x)$ and $u(x) = \sum_k u_k(x)$, with small perturbations $c_k, u_k \propto e^{\sigma t + ikx}$ and $k = 2\pi\, n/L$ ($n \in \mathbb{Z}$) being a discrete wave number. Moreover $c_{-k} = c_k^\star$ as well as $u_{-k} = u_k^\star$ holds because $c(x)$ and $u(x)$ are real fields. The resulting set of homogeneous linear equations yields a quadratic polynomial in σ as a solvability condition. If the real part of at least one of these solutions $\sigma_{1,2} = \kappa_{1,2} \pm i\omega$ becomes positive for some wave number k, the basic state $(c_0, 0)^T$ is said to be unstable. In case the imaginary part ω vanishes, the instability is stationary, whereas for finite ω an oscillatory bifurcation is met [35]. The motor parameter α is identified as the control parameter governing transitions from the homogeneous basic state to spatially and/or temporally modulated states.

The neutral curve $\alpha^S(k)$ characterizing the stationary bifurcation is obtained by solving the neutral stability condition $\kappa(k) = \sigma(k) = 0$ for the control parameter α. Defining $\Gamma = \eta d_0/2 + \nu c_0$ and $\Gamma' = \chi d_0 \Gamma \sin(k) - \eta k/2$, the instability threshold $\alpha_c^{S\pm}$ is given by the minimum of $\alpha^S(k)$,

$$\alpha^{S\pm}(k) = \frac{E\,\Gamma'}{\eta\,\delta\,\Gamma} \frac{k(1 + \cos k)}{\sin^2 k} \left[1 \pm \sqrt{1 + \frac{\delta\,\eta\,\Gamma\,k^2}{2\,E\,c_0\,\Gamma'^2}} \right], \tag{13}$$

which is located either at a vanishing critical wave number $k_c^S = 0$, thus implying a long-wavelength instability or at a finite wave number k_c^S that yields spatially periodic patterns. At the onset of the oscillatory bifurcation $\sigma_{1,2} = \pm i\omega$ and the critical value α_c^O of the control parameter is determined to be the minimum of the neutral curve

$$\alpha^O(k) = \alpha^F(k)\,(1 + E)\,/\,(1 - \zeta d_0 \Gamma) \tag{14}$$

with an appendant critical wave number $k_c^O = 0$. Herein

$$\alpha^F(k) = k^2 / \left[2c_0\,(1 - \cos k) \right] \tag{15}$$

is the neutral curve yielding the onset $\alpha_c^F \approx 1/c_0$ of the long-wavelength stationary instability in the absence of a network [30]. Within the limit $(d_0 \to 0)$ and disintegrating networks (i.e. $E \to 0$), the stationary thresholds $\alpha_c^{S\pm}$ disappear whereas the onset α_c^O of the oscillatory bifurcation converges to α_c^F with the frequency ω simultaneously vanishing. Therefore one regains for vanishing network densities the well-known long-wavelength, stationary bifurcation, for motor activities $\alpha > \alpha_c^F$, characteristic of oriented filament bundles [30].

A typical bifurcation scenario in the (α, E)-plane is sketched in Fig. 2(a). Altogether the elastic network adds to the long-wavelength bifurcation at α_c^F three new instability types as evinced by the diverse growth rates $\kappa_{1,2}(k)$ plotted as a function of the wave number k in Fig. 2(b) − (e). Provided that the rescaled barycentric transport coefficient χ is large enough, the elastic network increases the instability thresholds of the homogeneous filament distribution towards motor activities α higher than α_c^F, depending on E, either beyond the dashed or the dotted line in Fig. 2(a). If χ is too small the solid line abuts the threshold α_c^F and the only instability left is the long-wavelength stationary one, known already from oriented bundles without network elasticity [30], cf. Fig. 2(e). The same allegation holds for small network elasticities. Fig. 3 shows
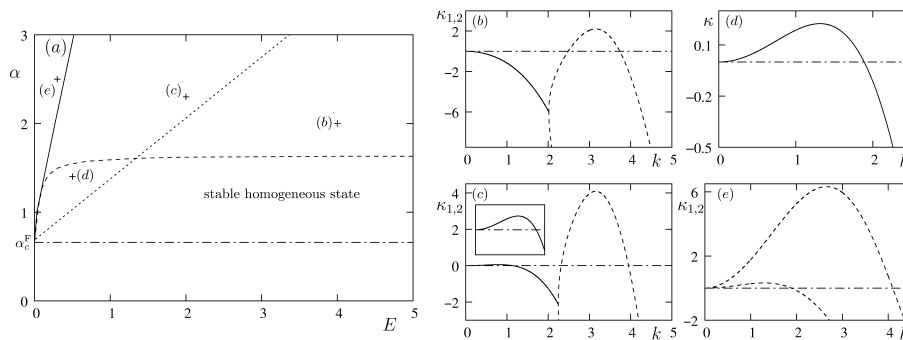
Figure 2. Part (a) shows the instability diagram in the (α, E)-plane for the parameter set $\chi = 2c_0 = 3\eta = 3$, $d_0 = 0.7$, $\delta = 2\mu = 4\nu = 0.2$. The dash-dotted line at α_c^F marks the threshold towards stationary contracted states for vanishing network densities. In the presence of a network, the instability of the homogeneous state is shifted either beyond the dotted or dashed line. Stiff networks with large E-values trigger a stationary, finite wave number instability, the characteristic growth rates $\kappa_{1,2}(k)$ being shown in (b). For smaller values of E an oscillatory long-wavelength instability is met, with the typical growth rate $\kappa(k)$ depicted in (d). E-values beneath the solid line yield a long-wavelength, stationary instability whose wave number dependent growth rates are depicted in (e), an instability type which is known from oriented filament bundles without network. Within the area between the solid and dotted lines lying beyond the dashed line, a long-wavelength, oscillatory instability competes with a finite wave number stationary one, with growth rates displayed in (c).

numerically obtained density profiles $c(x, t)$ of the free filaments beyond the respective instability thresholds as a function of x for a fixed system length L.

The diversification of the latter instability by the network is hence mostly driven by the barycentric transport imposed by the network upon the free filaments. If filament bundles with both orientations, i.e. comprising c^+- as well as c^--filaments, are considered instead of oriented ones, the barycentric transport coefficient χ becomes less relevant as the possibility of polarity sorting introduces an additional microscopic transport mechanism captured by the motor activity $\beta \neq 0$. In case of very stiff networks an increase in α leads to a short-wavelength, stationary instability whose wavenumber dependent growth rates are shown in Fig. 2(b). Within the nonlinear regime, this instability leads to stripe patterns as shown in Fig. 3(a). Looser polymer networks, corresponding to lower E-values, favor a transition from the homogeneous filament distribution to a long-wavelength, oscillatory mode characterized by the growth rate $\kappa(k)$ in Fig. 2(d) and rather irregular dynamics as depicted in Fig. 3(c). This oscillatory instability can compete with a short-wavelength stationary one, whose associated growth rates are displayed in Fig. 2(c). Within the nonlinear regime free filament density peaks, resulting from a coarsening process at an early stage, oscillate between extremal positions as shown in Fig. 3(b). This type of nonlinear behavior occurs in a large region of the (α, E)-plane bounded by the solid, dashed and dotted lines. For small rescaled elasticities E the long-wavelength, stationary instability characteristic of free oriented
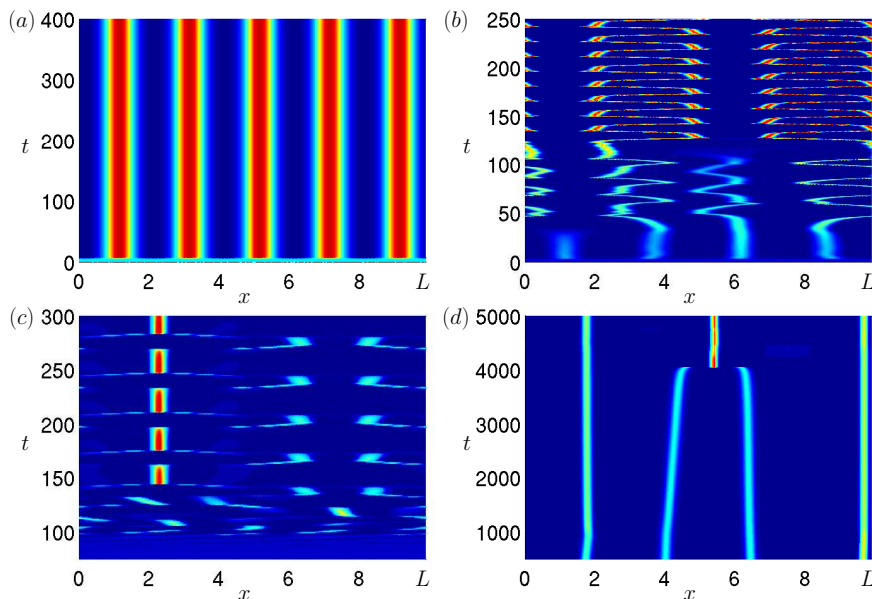
Figure 3. Numerically obtained profiles $c(x,t)$ of the free filament density with red color coding high and blue color coding low densities. Part (a) displays the density profile corresponding to the stationary finite-wavelength instability depicted in Fig. 2(b). In (b) (where, without changing the overall dynamical behavior, $\chi = 1.5$ has been chosen to perfectly highlight the oscillatory contributions) the competition of an oscillatory instability with a finite wave number stationary one is shown, the appendant growth rate being Fig. 2(c). Part (c) visualizes the oscillatory instability according to Fig. 2(d), and part (d) the stationary one, with the growth rate being pictured in Fig. 2(e).

filament bundles prevails in the presence of a network. The appendant nonhomogeneous stationary numerical solution is pictured in Fig. 3(d).

4. Patterns in an active viscoelastic bundle

Crosslinks among network filaments generally have a finite life time. If their life time is of the same time scale as the active transport processes, the static network becomes viscoelastic, a behavior that is incorporated in the model by a time constant $(\lambda + 2\mu)/\tau$ as done in a simple Voigt-Kelvin model. The associated equations read

$$\partial_t c \;\; = D\partial_x^2 c - \partial_x \left(J_{cc}^{++} + J_{dc}^{++} + J_u^{\chi} \right) , \tag{16a}$$

$$\gamma \, \partial_t u = \left[\, (\lambda + 2\mu) + \tau \, \partial_t \, \right] \partial_x^2 u + f_{cd}^{++} , \tag{16b}$$

wherein the frictional contributions ν and ζ have been omitted, a choice that does not alter the overall scenario. Moreover the viscoelastic contribution $\tau \partial_t u(x + \xi)$ to the force density $\left[(\lambda + 2\mu) + \tau \partial_t \right] \partial_x^2 u$ entering the barycentric flux (4) of the free filaments will be neglected subsequently as it would only quantitatively modify the existence domains of the encountered instability types. The equations can once again be rescaled using the dimensionless coordinates of the previous section with the supplement $\tau' = \tau/(\gamma \, \ell^2)$.
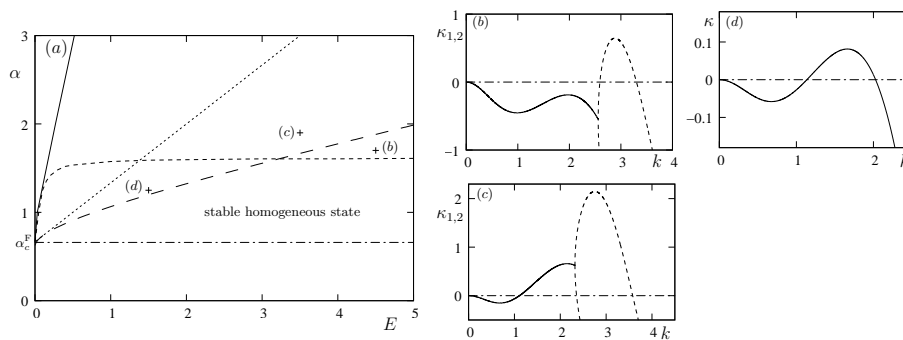
Figure 4. (*a*) Phase diagram in the (α, E)-plane for the parameter set used in Fig. 2 except that $\zeta = \nu = 0$ (w.l.o.g.) and $\tau = 1$. The dash-dotted line at α_c^{F} is the instability threshold without network. For stiff networks with large E the homogeneous state becomes unstable, beyond the dashed line, via a finite wave number, stationary bifurcation whose growth rates $\kappa_{1,2}$ are plotted in (*b*) as a function of the wave number k. In case of smaller E the latter state bifurcates through a finite wave number, oscillatory instability characterized by a typical growth rate shape depicted in (*d*). In between the dotted, dashed and long-dashed lines the short-wavelength, oscillatory instability competes with a stationary one, setting in at finite wave number, as evinced in Fig. 4(*c*) by the according growth rates $\kappa_{1,2}(k)$. The remaining areas within the (α, E)-plane exhibit exactly the same dynamics as in case of a non-viscoelastic network in Fig. 2(*a*).

A linear stability analysis analogous to the one performed in the last paragraph reveals that the viscoelasticity of the network additionally triggers beyond some critical motor activity α_c^{W}, lying at the minimum of the neutral curve

$$\alpha^{\mathrm{W}}(k) = \alpha^{\mathrm{F}}(k) \left(1 + E + k^2\tau\right) / \left(1 + k^2\tau\right) , \qquad (17)$$

a bifurcation to traveling (TW) or standing (SW) free filament density waves with critical wave number k_c^{W}. The corresponding generic growth rate is displayed in Fig. 4(*d*) as a function of the wave number k. Due to the network's viscoelasticity long-wavelength perturbations become always damped, provided that the elasticity E is large enough, as evinced by the growth rate shapes in Fig. 4(*b*)-(*d*). Additionally, as the total filament density - $\int dx\, [c(x) + d(x)] = \mathrm{const.}$ - is a conserved quantity for the investigated model all growth rates are diffusive in the long-wavelength limit. This mechanism proves to be utterly important since the coarsening process associated with a long-wavelength instability is suppressed and finite wavenumber TW and SW patterns are stabilized. Here the viscoelasticity of the network thus permits the filament-motor system to produce stable patterns. It is however known that long-wavelength modes yielded by conservation laws can render traveling or standing wave states unstable in the strongly nonlinear regime as shown e.g. in Ref. [36] for a model of mobile, charged ion channels embedded into a biomembrane.

Otherwise the phase diagram, Fig. 4(*a*), looks rather similar to the one discussed previously for elastic networks. The only differences are: Upon increasing the motor activity α, the homogeneous filament distribution now firstly is unstable against the
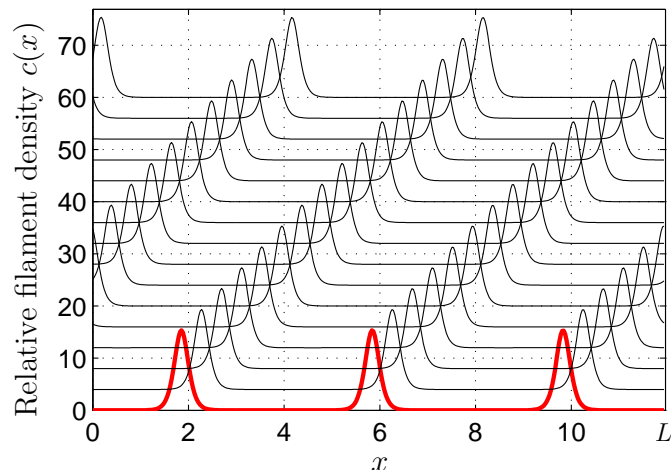
Figure 5. A numerically obtained traveling wave (TW) density profile $c(x)$ that corresponds to the growth rate displayed in $4(d)$. The red curve depicts the filament density profile at $t = 20$ whereby the black curves show its temporal evolution up to $t = 50$ by time steps of $\Delta t = 2$. The reduced control parameter $\varepsilon = \left(\alpha - \alpha_c^{\mathrm{W}}\right)/\alpha_c^{\mathrm{W}}$ evaluates to 0.3 whereby $\alpha_c^{\mathrm{W}} = 1.18$. The subcriticality of the bifurcation from the homogeneous free filament distribution to the displayed filament density wave results in the anharmonic wave form. The system length is $L = 12$.

aforesaid short-wavelength, oscillatory instability for small E-values, whereas large rescaled elasticities still favor a transition to a finite wave number stationary bifurcation with modes growing according to $\kappa_{1,2}(k)$ shown in Fig. 4(b). A further increase in α leads to a coupling of the latter instability to the finite wave number oscillatory one as may be deduced from the growth rate depicted in Fig. 4(c). Large rescaled elasticities E and finite τ-values generally favor the Hopf bifurcation to traveling or standing free filament density waves, which survive in the nonlinear regime as can be seen from Fig. 5. Within the limit $\tau \to \infty$ the onset α_c^{W} of the latter wave patterns, visualized by the long-dashed line in Fig. 4(a), abuts the stationary threshold α_c^{F} characteristic of free filament bundles. In fact, for $\tau \to \infty$, the force applied by motor mediated interactions to the network filaments is dissipated by prevalent, frictional effects within the network. Thus within this limit network strain cannot build up and the free filament dynamics is hardly influenced.

5. Mechanosensitivity

Although the long-wavelength, stationarry instability is already encountered in oriented fiber bundles lacking a (visco-)elastic network, where it is interpreted as a contracted state, it gains within the framework of the present (visco-)elastic model a striking new quality: its threshold, given by the minimum of Eq. (13), depends on both the mean network density d_0 and the network elasticity E. As does the stationary instability at finite wave number, the newly emerging oscillatory instabilities, that result from the

coupling of the free filament dynamics to the (visco-)elastic network also depend on both parameters d_0 and E as can be seen from α_c^O. This stipulates that the aforesaid density instabilities can be controlled through compression and dilation - either externally by applying a force or internally by molecular motor activity - of the elastic network or of the filament bundle in our one-dimensional case. Compressing or dilating the network alters the mean filament density d_0 of the network, thereby changes the self-organization process of the free filaments and might be used to rapidly switch between the different instability scenarios discussed throughout this work. Addressing pattern formation by compression or dilation of a biopolymer network thus seems to be effectively equivalent to steering pattern formation by modifying motor activity through ATP concentration. It is known that cell movement needs adhesion to the substrate to transduce force, and it might be speculated that such external forces via the mechanism described above interplay with the internal cytoskeleton structure: periodic contraction waves in lamellipodia [37], as well as spontaneous oscillations in a muscle bundle have been reported [38], where the bundle's elasticity might be relevant too.

6. Conclusions

Numerous experimental and theoretical studies have been devoted either to the mechanical properties of filament networks or to the molecular motor triggered self-organization of filaments. In this work we have investigated the influence of networks on the latter self-organization process by proposing a simple model that couples the active filament dynamics to an either purely elastic or viscoelastic filament network.

The cytoskeletal structures that attracted most attention in recent years were the aster and vortex patterns found in dilute reconstituted solutions [6, 7]. They have been successfully described as defect structures in the polar filament orientation field both by mesoscopic models in the dilute regime [11, 39] and macroscopic hydrodynamics models [9, 40]. To study the nonlinear dynamics of extended patterns and coarsening processes, the latter attempt proves difficult, since the generic approach is based on linear irreversible thermodynamics and yields only geometrical nonlinearities, while it is challenging to decide which additional nonlinearities are important [41]. Therefore we start from a model for the dilute regime, based on [5], and extend it by accounting for the elastic background by means of motor-induced filament-filament interactions only, which naturally yields the leading order, quadratic nonlinearities.

While stationary and propagating contractile states were reported previously in suspended filament-motor systems [4, 5, 31], new instability types and nonlinear competitions between the latter ones emerge when introducing the (visco-)elastic network. Especially, in the viscoelastic case, traveling and standing waves can be stabilized for specific elastic constants of the network. Moreover, all mentioned pattern forming processes are rendered mechanosensitive through the coupling to the network: the states as well as their onset crucially depend on the network density, elasticity and viscoelastic time constant, all these parameters being naturally relevant as a cell is

subjected to external forces and continuously reorganizes its cytoskeleton.

Various generalizations of this model should be considered in the future: one relevant and interesting point is to account for a finite lifetime of the crosslinkers and describing the system at timescales much larger than the average crosslinking time. First, the two-fluid separation has then to be genaralized by transitions rates between 'free' and 'network' filaments, naturally introducing the finite lifetime into the problem. As discussed above, this also allows the network to become anisotropic, even in one dimension. Second, on these time scales also the network part of the model becomes a viscoelastic fluid rather than a viscoelastic solid and a Maxwell-like model, as suggested in the framework of Ref. [40], should be more appropriate.

Secondly, the current one-dimensional model might be generalized to higher dimensions. The methods how to achieve this are principally known [8, 10, 11]. In the case of quasi-permanent crosslinkers, this would also be the first step towards the active elastomer, since the broken symmetry variable of the polar filament orientation should nontrivially couple to the (visco-)elastic field [42]. In forthcoming work we will also show that pattern formation can be conceived as an instrument to stiffen (visco-)elastic filament networks.

Acknowledgments

Appendix A. Derivation of J_1 and J_2

The general idea of the derivation of the active currents $J_{1,2}$ is as follows: Starting from two-filament interactions, one formulates the micro-force balance for the involved filaments, disregarding inertia terms. Since the system is considered to be embedded in a solvent, the local frictional force $F_f = \eta \dot{x}$ of a filament with the solvent suggests the associated currents $J(x,t) = c(x,t)\dot{x}$ to be

$$ J(x,t) = \frac{F_f}{\eta} c(x,t) \,. \tag{A.1} $$

In the case of two free plus-oriented filaments, the force balance implies

$$ \eta \dot{x}_a - F_{act,a} = 0 \quad \text{and} \quad \eta \dot{x}_b - F_{act,b} = 0 \,, \tag{A.2} $$

with $F_{act,a}, F_{act,b}$ being the active forces exerted by the motor on the two filaments, respectively (see Fig. A1(a)). Since no external forces are involved, the center of mass of the two filaments is invariant, leading to $F_{act} = F_{act,a} = -F_{act,b}$. Each force exerted on one filament by the motor is balanced by an opposing force acting on the other filament and both filaments cover the same distance Δx.

Eq. (A.1) then leads to $J_{cc}^{++} = \frac{1}{\eta} F'_{act} c^+(x,t)$, with F'_{act} being the representation of F_{act}
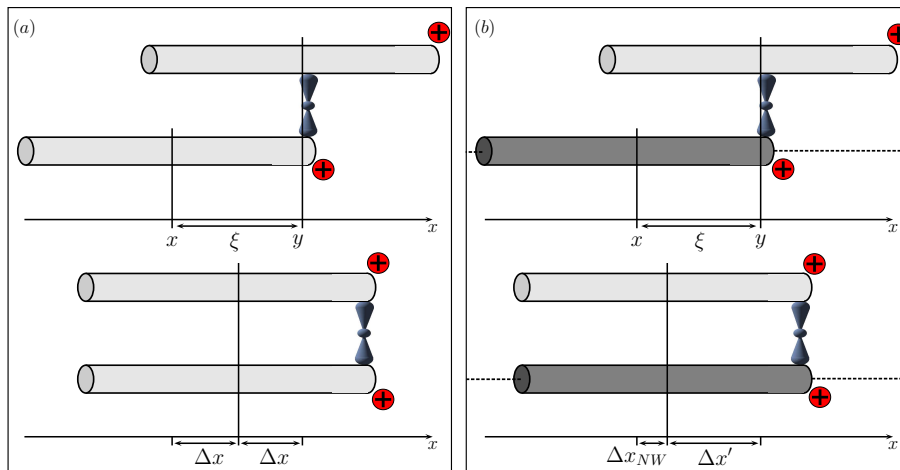
Figure A1. (*a*) Movement of two plus-directed free filaments coupled by a motor complex. Since no external forces are involved, the center of mass is invariant and both filaments are displaced by Δx. (*b*) Interaction of a free filament (light gray shaded) and a network filament (dark gray shaded) with their plus end pointing to positive x–direction. Since the elastic restoring force enters the force balance the displacement of the network filament Δx_{NW} is smaller than in the case of two interacting free filaments. Reciprocally the displacement of the free filament $\Delta x'$ is larger. Consequently the center of mass is not invariant any more.

in the mean field. Given that an overlap of the two filaments is a precondition for the active interaction and that due to force balance the forces F_{act} have to obey distinct symmetry relations the currents are given by Eq. (2*a*). For a more detailed and rigorous derivation we refer to Ref. [30].

However the situation is thoroughly changed if a free filament interacts with a network filament, leading to

$$\eta \dot{x}_{NW} = F_{act,b} + F_{elast} \tag{A.3}$$

as the equation of motion for the network filament, with F_{elast} being the elastic restoring force. Consequently the distance $\Delta x'$ covered by the free filament is larger than in the case without network (Δx), whereas the distance Δx_{NW} the network filament covers during an active interaction is smaller resulting in an effective barycentric transport (see Fig. A1(b)). Since the displacement of the free filament and the network filament are counter-directed,

$$x' - x_{NW} = 2x \tag{A.4}$$

applies here. Taking the derivative with respect to t on both sides and inserting Eq. (A.2) and $F_{act,a} = -F_{act,b}$ from above, gives an equation for $\dot{x}'$ which can be used to calculate the associated current

$$J_2^{++} = \frac{1}{\eta} \left(F'_{act} + F'_{elast} \right) c^+(x,t) = J_{dc}^{++} + J_u^{\chi,++} . \tag{A.5}$$

While in the mean field the current J_{dc}^{++} again takes the form of Eq. (3*a*), the current $J_u^{\chi,++}$ is due to the viscoelastic force density entering the force balance. It virtually

transmits the viscoelastic force density to the free filament. Considering a network plus–filament at $x + \xi$ and a free filament at x this gives rise to

$$J_u^{\chi,++} = \int_{-\ell}^{\ell} d\xi \left[\frac{\chi}{\eta} \left[(\lambda + 2\mu) + \tau \partial_t \right] \partial_x^2 u(x + \xi) \right] d^+(x + \xi) c^+(x) . \quad (A.6)$$

Together with $d^+ = d^- = d/2$ and $J_u^\chi = J_u^{\chi,++} + J_u^{\chi,+-}$ one finally receives

$$J_u^\chi = \int_{-\ell}^{\ell} d\xi \left[\frac{\chi}{\eta} \left[(\lambda + 2\mu) + \tau \partial_t \right] \partial_x^2 u(x + \xi) \right] d(x + \xi) c^\pm(x) \quad (A.7)$$

as the current associated with the barycentric transport.

References

[1] B. Alberts *et al.*, *Molecular Biology of the Cell*, Garland Publishing, New York (2001).
[2] J. Howard, *Mechanics of Motor Proteins and the Cytoskeleton*, Sinauer, Sunderland (2001).
[3] K. Takiguchi, J. Bio. Chem. **109**, 520 (1991).
[4] H. Nakazawa and K.Sekimoto, J. Phys. Soc. Jpn. **65**, 2404 (1996).
[5] K. Kruse and F. Jülicher, Phys. Rev. Lett. **85**, 1778 (2000).
[6] R. Urrutia R. *et al.*, Proc. Natl. Acad. Sci. USA **88**, 6701 (1991).
[7] F. J. Nedelec *et al.*, Nature **389**, 305 (1997).
[8] T. B. Liverpool and M. C. Marchetti, Phys. Rev. Lett. **90**, 138102 (2003).
[9] K. Kruse, *et al.*, Phys. Rev. Lett. **92**, 078101 (2004).
[10] F. Ziebert and W. Zimmermann, Eur. Phys. J. E **18**, 41 (2005).
[11] I. S. Aranson and L. S. Tsimring, Phys. Rev. E **71**, 050901 (2005).
[12] A. Bausch and K. Kroy, Nature Physics **2**, 231 (2006).
[13] J. Wilhelm and E. Frey, Phys. Rev. Lett. **91**, 108103 (2003).
[14] D. A. Head, A. J. Levine and F. C. MacKintosh, Phys. Rev. Lett. **91**, 108102 (2003).
[15] C. Storm, *et al.*, Nature **435**, 191 (2005).
[16] C. Heussinger and E. Frey, Phys. Rev. Lett. **97**, 105501 (2006).
[17] R. Tharmann, M.M.A.E. Claessens and A. R. Bausch, Phys. Rev. Lett. **98**, 088103 (2007).
[18] L. LeGoff, F. Amblard and E.M. Furst, Phys. Rev. Lett. **88**, 018101 (2002).
[19] D. Mizuno, *et al.*, Science **315**, 370 (2007).
[20] D. M. Smith *et al.*, Biophys. J. **93**, 4445 (2007).
[21] F. Backouche, *et al.*, Phys. Biol. **3**, 264 (2006).
[22] F. Ziebert, I. S. Aranson and L. S. Tsimring, New J. Phys. **9**, 421 (2007).
[23] J. F. Joanny, K. Kruse, F. Jülicher and J. Prost, New J. Phys. **9**, 422 (2007).
[24] A. L. Hitt, A. R. Cross and J. R. C. Williams, J. Bio. Chem. **265**, 1639 (1990).
[25] P. Dalhaimer, D. E. Discher and T. C. Lubensky, Nature Phys. **3**, 354 (2007).
[26] H. R. Brand, H. Pleiner and P. Martinoty, Soft Matter **2**, 182 (2006).
[27] F. Brochard and P. G. De Gennes, Macromolecules **10**, 1157 (1977).
[28] S. T. Milner, Phys. Rev. E **48**, 3674 (1993).
[29] F. Ziebert and W. Zimmermann, Phys. Rev. E **70**, 022902 (2004).
[30] K. Kruse and F. Jülicher, Phys. Rev. E **67**, 051913 (2003).
[31] K. Kruse, S. Camalet and F. Jülicher, Phys. Rev. Lett. **87**, 138101 (2001).
[32] L. D. Landau and E. M. Lifshitz, *Lehrbuch der theoretischen Physik, Band 7, Elastizitätstheorie*, Akademie Verlag, Berlin (1975).
[33] R. B. Bird, R. C. Armstrong and O. Hassager, *Dynamics of Polymeric liquids, Vol. 1*, John Wiley & Sons (1977).
[34] R. M. Christensen, *Theory of Viscoelasticity*, Dover Publications, Mineola (1982).
[35] M. C. Cross and P. C. Hohenberg, Rev. Mod. Phys. **65**,851, (1993).

[36] R. Peter and W. Zimmermann, Phys. Rev. E **74**, 016206, (2006).

[37] G. Giannone, *et al.*, Cell **116**, 431 (2004).

[38] H. Fujita and S. Ishiwata, Biophys. J. **75**, 1439 (1998).

[39] I. S. Aranson and L. S. Tsimring, Phys. Rev. E **74**, 031915 (2006).

[40] K. Kruse, *et al.*, Eur. Phys. J. E **16** 5 (2005).

[41] F. Jülicher, *et al.*, Phys. Reports **449**, 3 (2007).

[42] H. R. Brand and H. Pleiner, Physica A **208**, 359 (1994).